Characterization, physicochemical and photo-stability of a co-crystal involving an antibiotic drug, nitrofurantoin, and 4-hydroxybenzoic acid

Venu R. Vangala,*[a] Pui Shan Chow,[a] and Reginald B. H. Tan*[a,b]

[a] *Crystallisation and Particle Science, Institute of Chemical and Engineering Sciences, A*STAR (Agency for Science, Technology and Research), 1 Pesek Road, Jurong Island, Singapore, 627833. E-mail: venugopal_vangala@ices.a-star.edu.sg*

[b] *Department of Chemical & Biomolecular Engineering, National University of Singapore, 10 Kent Ridge Crescent, Singapore 117576. E-mail: reginald_tan@ices.a-star.edu.sg*

Electronic Supplementary Information (ESI)
(16 pages)

Table of contents

Experimental

Materials. NF (β-form) commercial material with purity of >99% was purchased from Sigma Aldrich. The reactants 4-HBA, 3-HBA, 2-HBA (SA), solvents and other reagents were obtained from Alfa-Aeser commercial suppliers and used as received.

Solid-state (neat and solvent drop) grinding experiments. These were performed on a Retsch Mixer Mill model MM301 with 10 mL stainless steel grinding jars and one 7 mm stainless steel grinding ball at a rate of 20 Hz for 30 min. Experiments were carried out with 119 mg (0.5 mmol) of NF and corresponding stoichiometric amount of 4HBA (69 mg, 0.5 mmol) for 1:1 studies. Accordingly, necessary amount of each reactant (0.5 mmol vs 1 mmol) have been taken for either 1:2 or 2:1 molar ratio for the neat and solvent drop grinding (NG, SDG) studies. While solvent-drop grinding (SDG) experiments were conducted by adding *ca.* 0.05 ml (2 drops from a pipette) of acetonitrile to the reactants prior to the grinding. The resulting powder samples were analyzed by PXRD. The external temperature of the grinding jar at the end of grinding did not exceed 30 °C.

Preparation of NF-4HBA (1:1) by solution crystallization. NF-4HBA (1:1) prepared in several batches from 2 mmol quantities of reactants each time from acetonitrile by evaporative crystallization at the ambient conditions.

Powder X-ray diffraction (PXRD). PXRD data were collected in Bragg-Brentano geometry with a Bruker D8 Advance (Bruker AXS GmbH, Germany) X-ray powder diffractometer equipped with Cu-Kα radiation (λ = 1.54056 Å) source, a Nickel-filter, 0.3° divergence slit, a linear position sensitive detector (Vantec-1) and an Anton Paar Model HTK 1200 High Temperature Chamber. The diffractometer was operated at 35 kV and 40 mA. The sample was loaded onto a glass circular sample holder and levelled with a glass slide. The sample was scanned within the scan range of 2θ = 5° to 50° continuous scan, at a scan rate of 2 deg min^{-1}.

Thermal Analysis. Differential scanning calorimetry (DSC) was performed with a Perkin Elmer, Diamond DSC with Autosampler. Crystals taken from the mother liquor were blotted dry on a filter paper and manually ground to obtain fine powder. 2-5 mg of each sample was placed in crimped sample pan. The sample was heated from 30 to 300 °C at a heating rate of 10 °C/min. The samples were purged with a stream of flowing nitrogen at 20 mL/min.

Thermogravimetric analysis (TGA) was performed on a TA instruments, TGA Q500 thermogravimetric analyzer. Approximately 10 mg of the sample was added to an alumina crucible. The samples were heated over the temperature range of 30 to 350 °C at a heating rate of

10 °C/min. The samples were purged with a stream of flowing nitrogen throughout the experiment at 40 mL/min.

Differential thermal analysis (DTA) and differential scanning calorimetry (DSC) by SDT 2960, TA instruments have been used for storage stability studies. About 5 mg of the sample was taken in a crucible and heated over the temperature range of 30 to 350 °C at heating rate of 10 °C/min.

Infrared (IR) spectroscopy. Transmission infrared spectra of the solids were obtained using a Fourier-transform infrared spectrometer (Bio-Rad, FTS 3000MX IR spectrometer). Typically, ~25 mg of the sample was ground with KBr in an agate mortar and pressed with a steel die into a pellet. The FT-IR spectra were collected for 64 scans at 4 cm^{-1} resolution.

Raman spectroscopy. The dispersive Raman microscope employed in this study was a JY Horiba LabRAM HR equipped with a confocal microscope, liquid-nitrogen-cooled charge-coupled device (CCD) and a multichannel detector (256 pixels × 1024 pixels). The NIR 784.8 nm argon ion laser was selected to excite the Raman scattering. The Raman shift range acquired was in the range of 100-1700 cm^{-1} with spectral resolution 1.7-2 cm^{-1}.

Single crystal X-ray diffraction. Single crystal of suitable quality was chosen under a Leica microscope and placed on a fibre needle which was then mounted on the goniometer of the X-ray diffractometer. The crystal was purged with a cooled nitrogen gas stream at 110 K throughout the data collection. X-ray reflections were collected on a Rigaku Saturn CCD area detector with graphite monochromated Mo-Kα radiation (λ = 0.71073 Å). Data were collected and processed using CrystalClear (Rigaku) software. Structures were solved by direct methods and SHELX-TL was used for structure solution and least-squares refinement. The non-hydrogen atoms were refined anisotropically. All hydrogen atoms were fixed at idealized positions except for the N–H and O–H hydrogens which were located from the difference Fourier map and allowed to ride on their parent atoms in the refinement cycles. Details of hydrogen bonding interations present in NF-4HBA are given in Table S2.

Physicochemical storage stress studies. Relative humidity (RH) conditions were achieved in the sealed glass desiccators containing P_2O_5 for <10% RH and appropriate saturated aqueous salt solutions for other RH conditions: K_2SO_4 for 96-97%; NaCl for 75%; NaBr for 57% and $MgCl_2$ for 33%. Periodically, RH conditions were monitored with humidity-indicator pens. The required temperatures ca. 24 °C and 40 °C were obtained upon storage of the sealed desiccators in an oven. While accelerated stability condition, 40 °C and 75% RH, was achieved in ESPEC SH-241 temperature and humidity chamber. Both NF (β-form) commercial material and NF-4HBA (1:1) were dried at 30 °C and 20 mbar for 24 h. Subsequently, ~200 mg of sample was subjected to incubation studies in an open vial for the each time point and in various storages. Analyses of the product phases were carried out by PXRD and for selected samples by SEM. NF assays were determined by HPLC.

Scanning Electron Microscopy. The electron microscopy measurements were performed at a JEOL JSM-6700F field emission scanning electron microscope (SEM).

Photo-stability studies. Photo-stability was carried out using Intelli-Ray shuttered UV flood light. The wavelength of the artificial UV light was in the range of 315 and 400 nm. NF and NF-4HBA (1:1) solid-state powder samples have been sieved (<300 μm) and subjected for a study. UV exposed time points studied were being 1, 3, 6, 12, 18, 24, 48, 72 and 168 h. Each time point has been analyzed by HPLC.

High Performance Liquid Chromatography (HPLC). The NF content was analyzed by an HPLC (Agilent 1100 series) equipped with an Agilent Extend-C18 column (3.5 μm, 4.6 mm x 150 mm). Next, the powder was accurately measured for 30 μg ml^{-1} ethanol solution. Separations were conducted using the mobile phase of a mixture of water and acetonitrile (10:90) in a gradient elution at 1 mL/min. An injected volume of 2 μL was used. Detection wavelength in the UV–visible was set at 375 nm. A linear calibration curve was constructed at a concentration range of approximately 5-50 μg/mL and with R^2 of 0.99 (n=3).

Fig. S1 Solid-state neat (NG) and solvent drop grinding (SDG) studies attempted with NF (β-form) and 2HBA in different molar ratios: (a) 1:1 NG, (b) 1:1 SDG, (c) and (d) 1:2, (e) and (f) 2:1, respectively. Acetonitrile was used for all SDG studies. Simulated PXRD patterns of NF polymorphic forms and 2HBA compared against the grinding results. Grinding studies show that the PXRD patterns either match with 2HBA , NF (β-form) or NF-H_2O (Form-II).

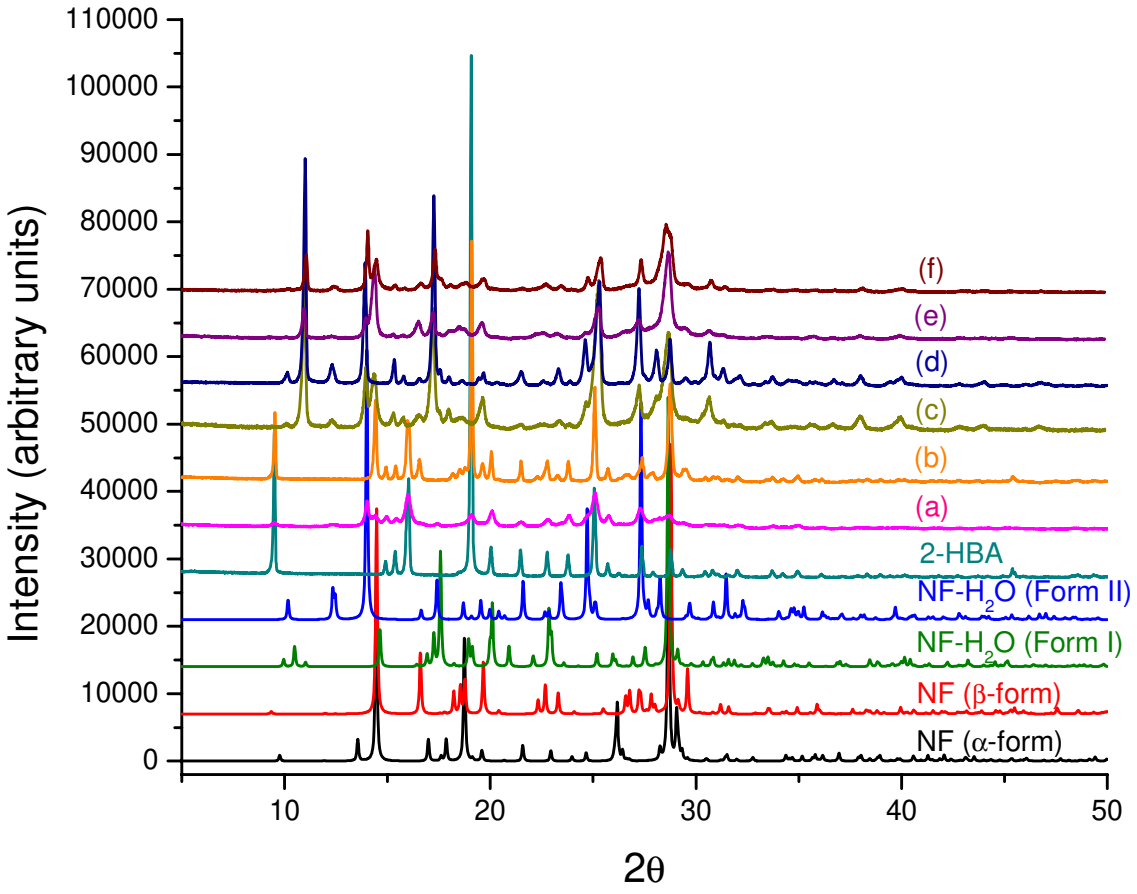

Fig. S2 Solid-state neat (NG) and solvent drop grinding (SDG) studies attempted with NF (β-form) and 3HBA in different molar ratios: (a) 1:1 NG, (b) 1:1 SDG, (c) and (d) 1:2, (e) and (f) 2:1, respectively. Acetonitrile was used for all SDG studies. Simulated PXRD patterns of NF polymorphic forms and 3HBA compared against the grinding results. Grinding studies show that the PXRD patterns either match with 3HBA , NF (β-form) or NF-H_2O (Form-II).

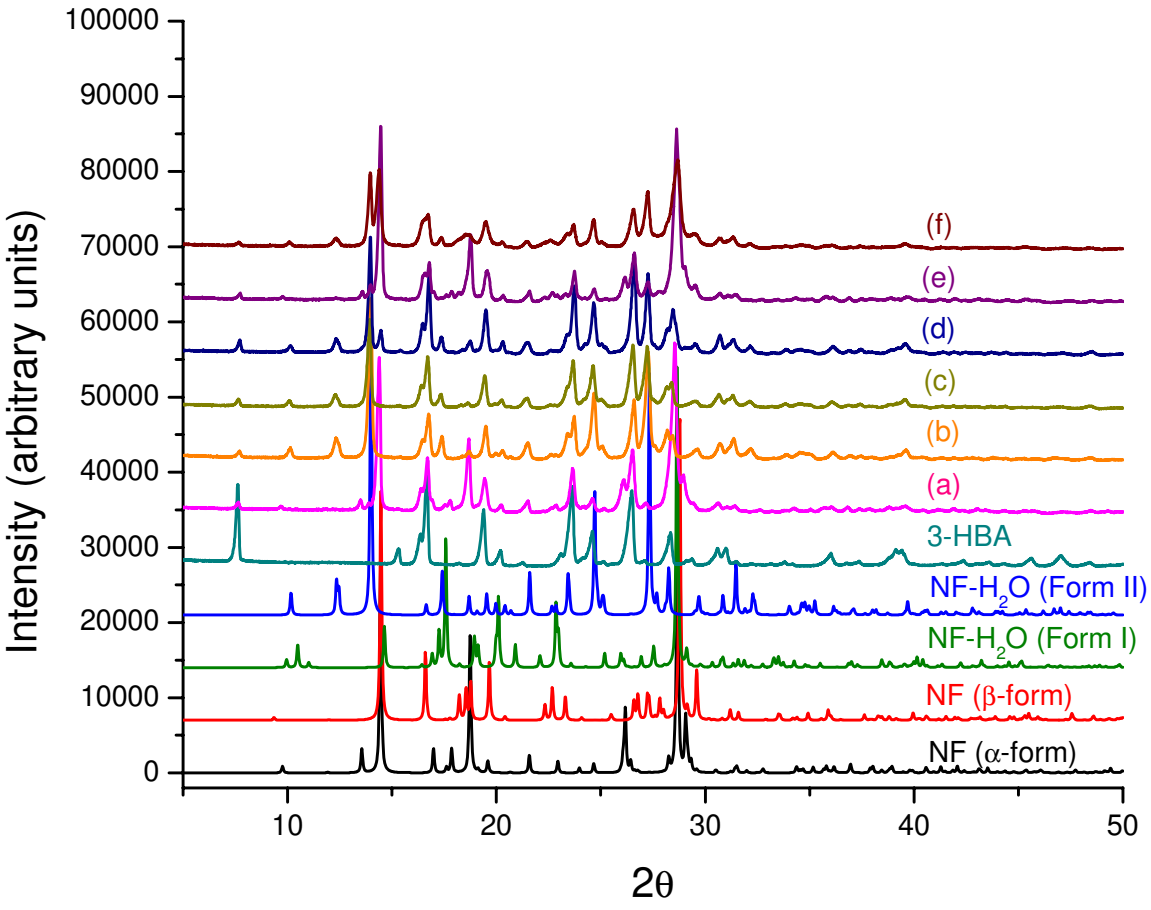

Fig. S3 Solid-state neat (NG) and solvent drop grinding (SDG) studies conducted with NF (β-form) and 4HBA in different molar ratios: (a) 1:1 NG, (b) 1:1 SDG, (c) and (d) 1:2, (e) and (f) 2:1 stoichiometric ratios respectively. Acetonitrile was used for all SDG studies. Simulated PXRD patterns of NF polymorphic forms and 4HBA compared against the grinding results. Grinding studies showed that there was a unique phase formation in all the molar ratios aside NF-H_2O (Form-II).

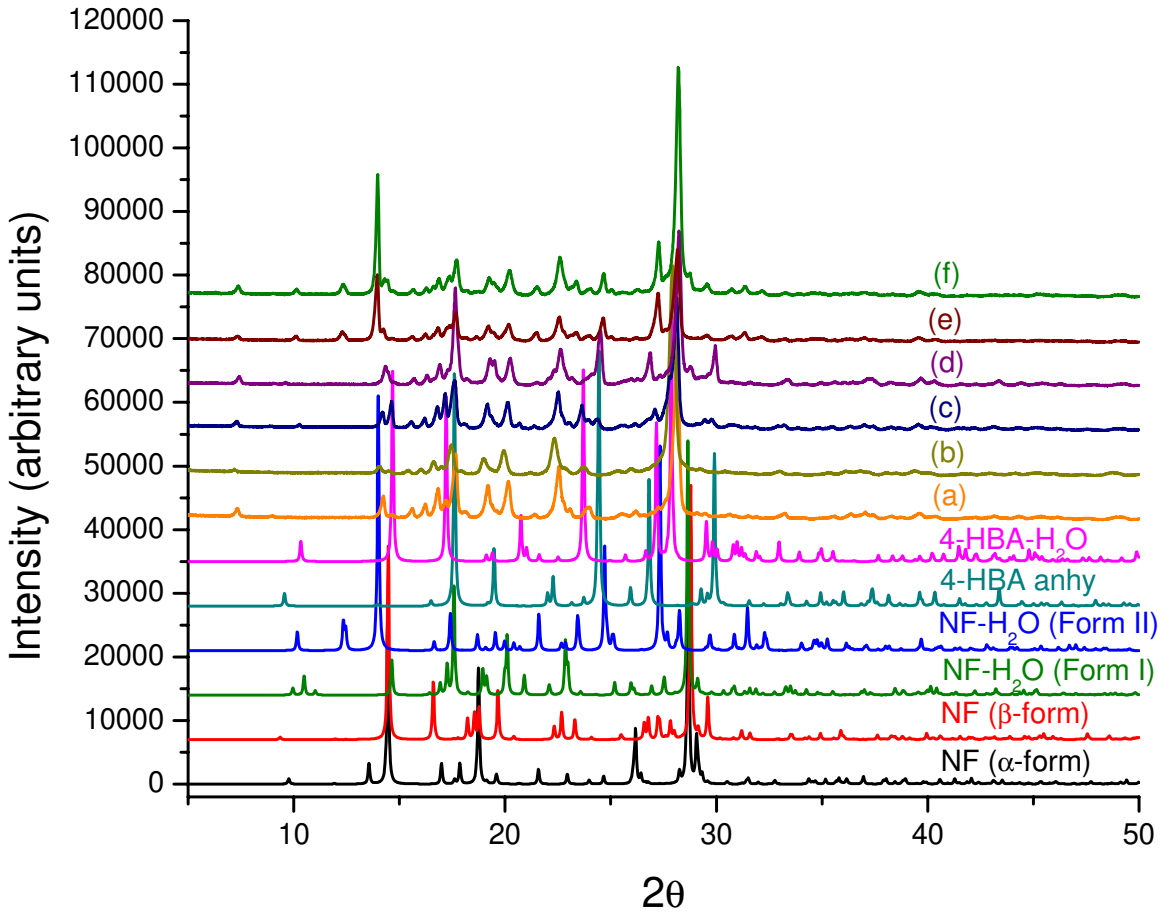

Fig. S4 DSC traces for NF, 4HBA and (1:1) cocrystal of NF-4HBA (30 - 275°C).

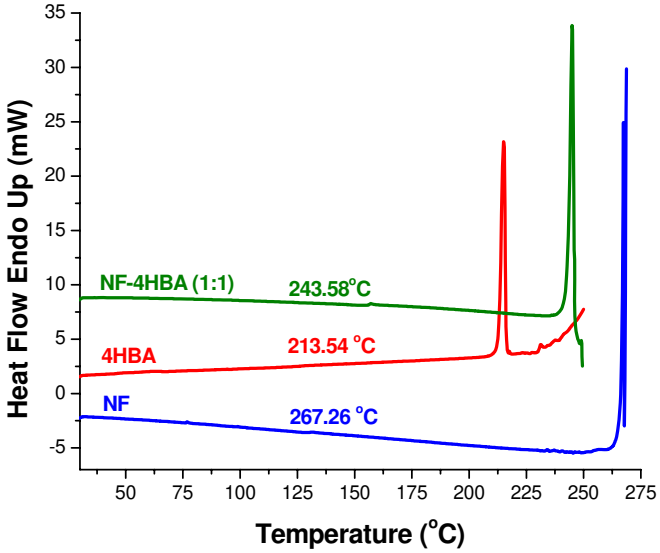

Fig. S5 TGA profiles for NF, 4HBA and NF-4HBA. Weight loss is negligle until 180 °C.

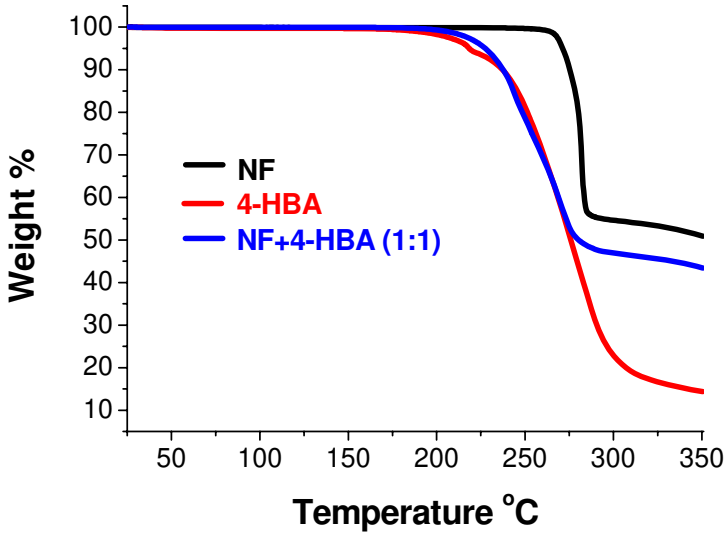

Fig. S6 IR spectral lines for NF, 4HBA and NF-4HBA. Note the distinctive IR pattern for NF-4HBA.

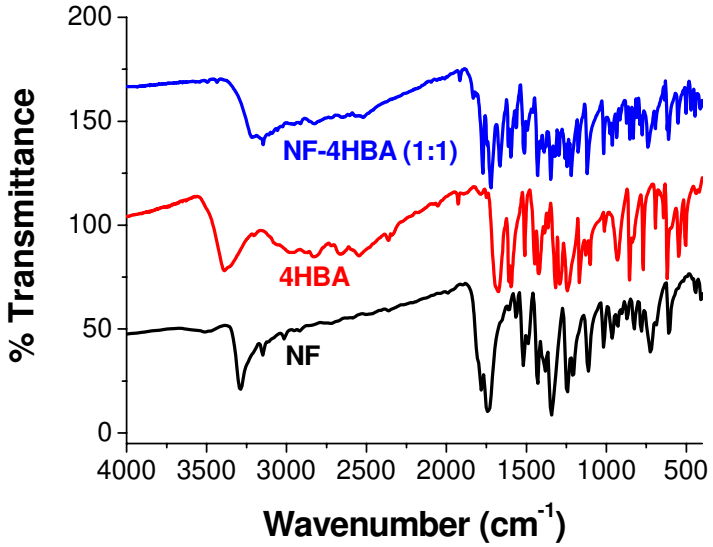

Fig. S7 Raman spectral lines for NF, 4HBA and NF-4HBA. Note the distinctive Raman pattern for NF-4HBA

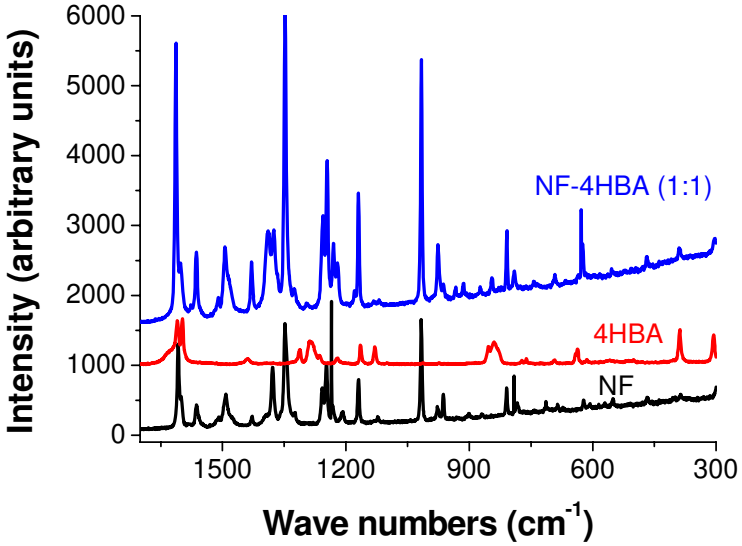

Table S1 Assignment of characteristic Raman bands for NF, 4HBA and NF-4HBA respectively.

NF (cm-1)		NF-4HBA (cm-1)		4HBA (cm-1)		Band assignment[a]
IR	**Raman**	**IR**	**Raman**	**IR**	**Raman**	
3288	-	3213	-			ν N–H (imide)
1323	1325	1321	1324			β N–H (imide)
723	714	736	714			γ N–H (imide), weak in Raman
1781	1774	1773	1769			ν C=O (imide; in-phase)
1735	-	1721	-			ν C=O (imide; out-of-phase)
741/723	742	737	743			γ C=O (imide)
571	571	576	577			γ C=O (imide) weak
1209	1208	-	-			ν_{as} C–O (Furanyl)
929	931	935	932			ν C–O (Furanyl)
1343	1349	1346	1347			ν_s NO_2
1564	1564	1563	1563			ν_{as} NO_2
809	810	808	808			ν_{sciss} NO_2
747	746	736	743			ω NO_2
552	552	549	554			ρ NO_2
		-	-	3387	-	ν O–H (phenolic)
		3197	-	3203	-	ν O–H (acid)
		1665	-	1675	-	ν C=O (acid)
		1614	1613	1610	1609	ν_s C=C
		1297	1295	1290	1287	C–OH (aromatic)
		1245	1230	1240	1264	ν C–O (aromatic)
		1217	1220	-	1220	ν_{as} C–OH (acid)
		1170	1169	1165	1160	ν C(aromatic)-COO (neutral)

[a]ν = streching, β = in-plane deformation, γ = out-of-plane deformation, ω = wagging and ρ = rocking.

Fig. S8 ORTEP plot at the 50% probability level. Asymmetric unit constitutes one independent molecule each of NF and 4HBA.

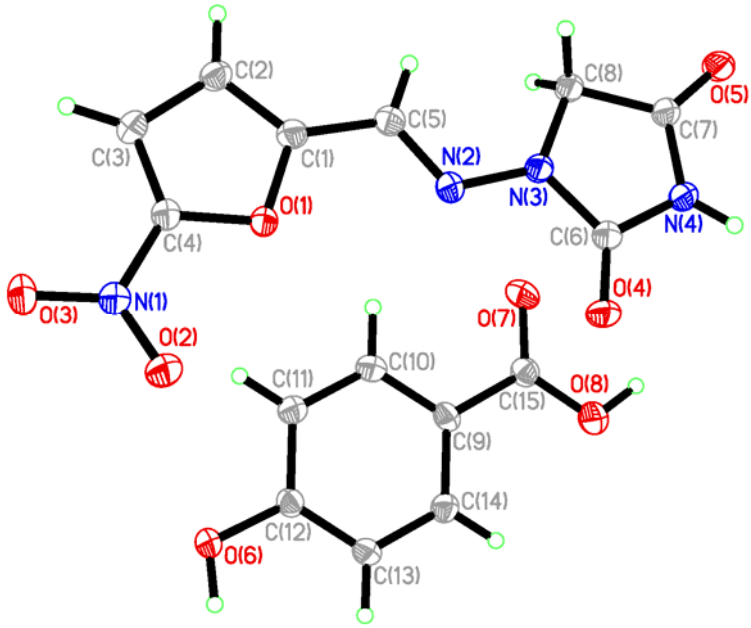

Table S2 Hydrogen bond geometries for 1:1 co-crystal of NF-4HBA.[a]

D–H···A	*d*(H···A)/ Å	*d*(D···A)/ Å	∠(D–H···A)/ °	Symmetry code
N–H···O	1.89	2.8920(19)	171	-1+x,y,z
O–H···O	1.70	2.6737(17)	171	1+x,y,z
O–H···O	1.62	2.5962(19)	172	-x,1-y,-z
C–H···O	2.28	3.050(2)	126	x,-1+y,z
C–H···O	2.77	3.787(2)	157	2-x,-1/2+y,1/2-z
C–H···O	2.21	3.286(2)	171	x,-1+y,z
C–H···O	2.60	3.683(2)	175	x,-1+y,z
C–H···O	2.58	3.473(2)	139	1-x,-1/2+y,1/2-z
C–H···O	2.38	3.414(2)	158	1+x,y,z
C–H···O	2.53	3.279(2)	125	1+x,1+y,z

[a]N–H, O–H and C–H geometries were normalized to 1.009, 0.983 and 1.083 Å, respectively.

Fig. S9 Co-crystal layered packing, view down the *b*-axis, was stabilized by π-π stacking. The C–H···O hydrogen bonds confer additional stability to the layers.

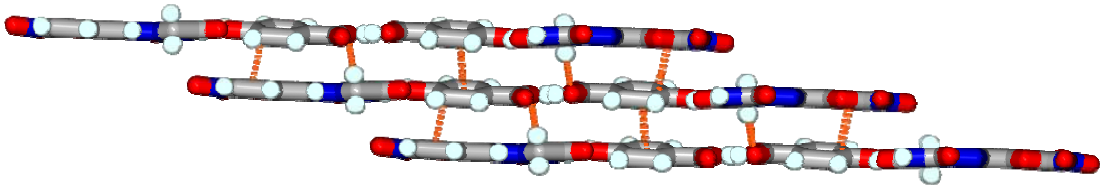

Fig. S10 Co-crystal packing along the *c*-axis. Independent layers color coded as purple and green. Notice the π-π stacking interactions between 4HBA–furanyl ring of NF ($\pi_{c=c}\cdots\pi_{c=c}$) and also within 4HBA ($\pi_{centroid}\cdots\pi_{c=c}$) in an antiparallel fashion and all other hydrogen bonds were omitted for a clarity.

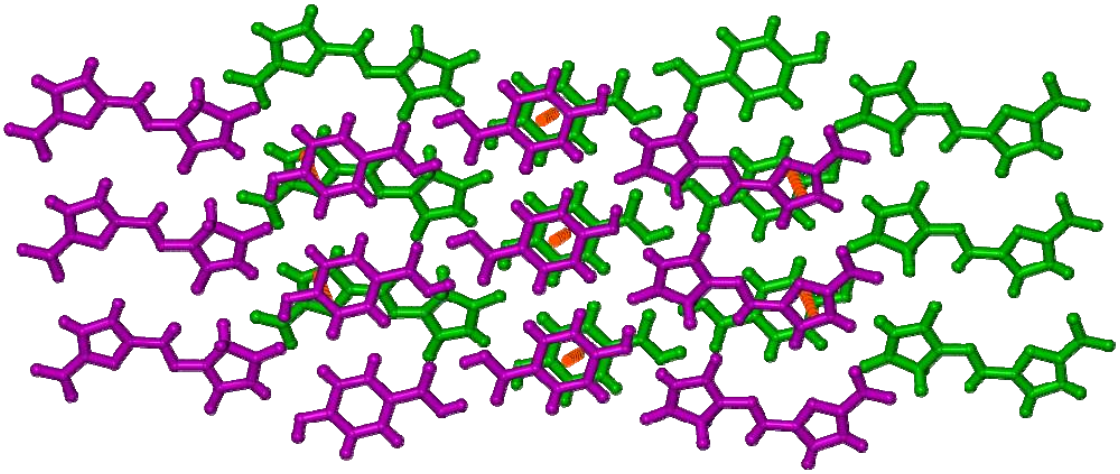

Fig. S11 (a) NF and (b) NF-4HBA (1:1) samples were incubated at 24 °C and <10% RH during 13 weeks. Product phases did not show detectable phase changes in PXRD.

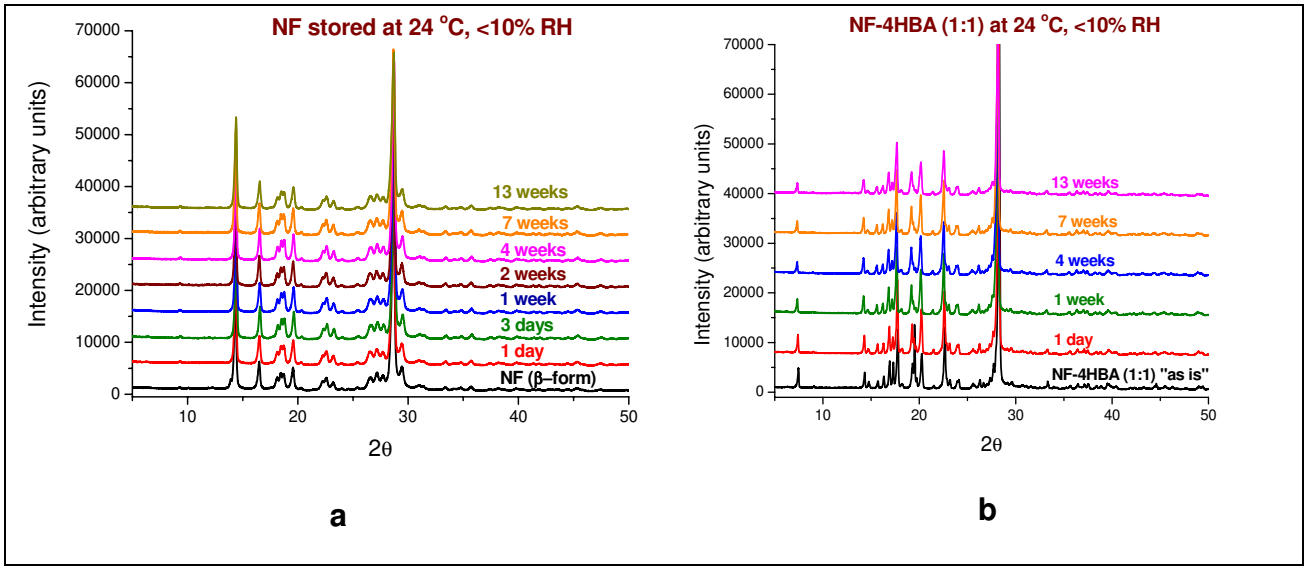

Fig. S12 (a) NF and (b) NF-4HBA (1:1) samples were incubated at 24 °C and 33% RH during 13 weeks. Product phases did not show detectable phase changes in PXRD.

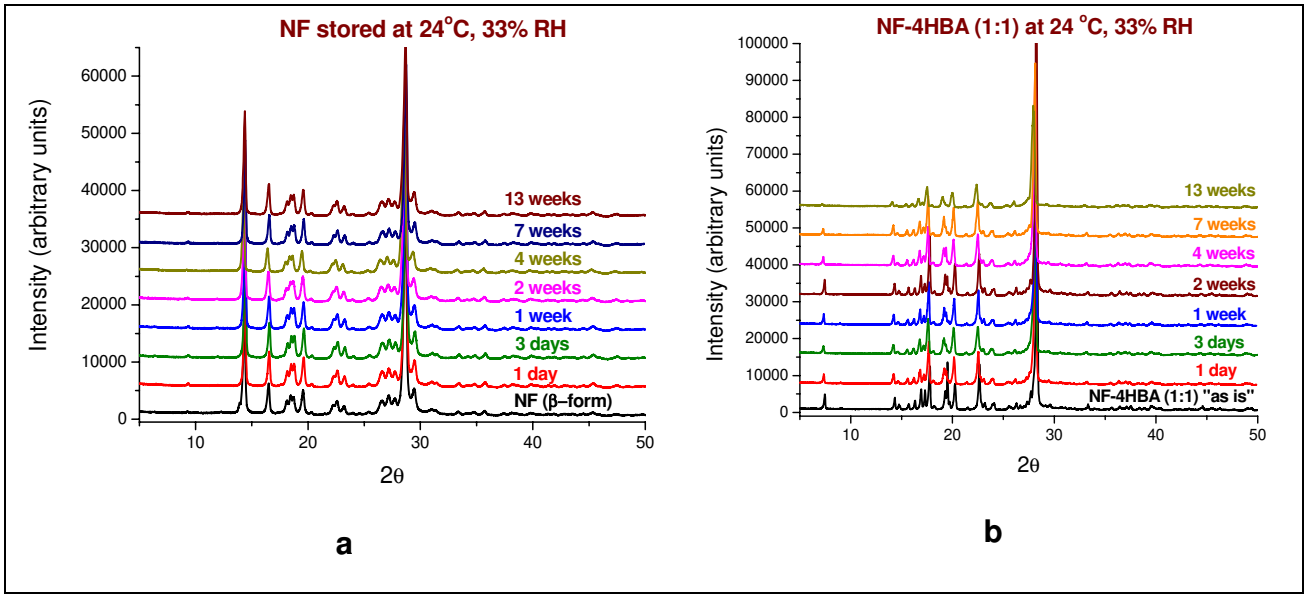

Fig. S13 (a) NF and (b) NF-4HBA (1:1) samples were incubated at 24 °C and 57% RH during 13 weeks. Product phases did not show detectable phase changes in PXRD.

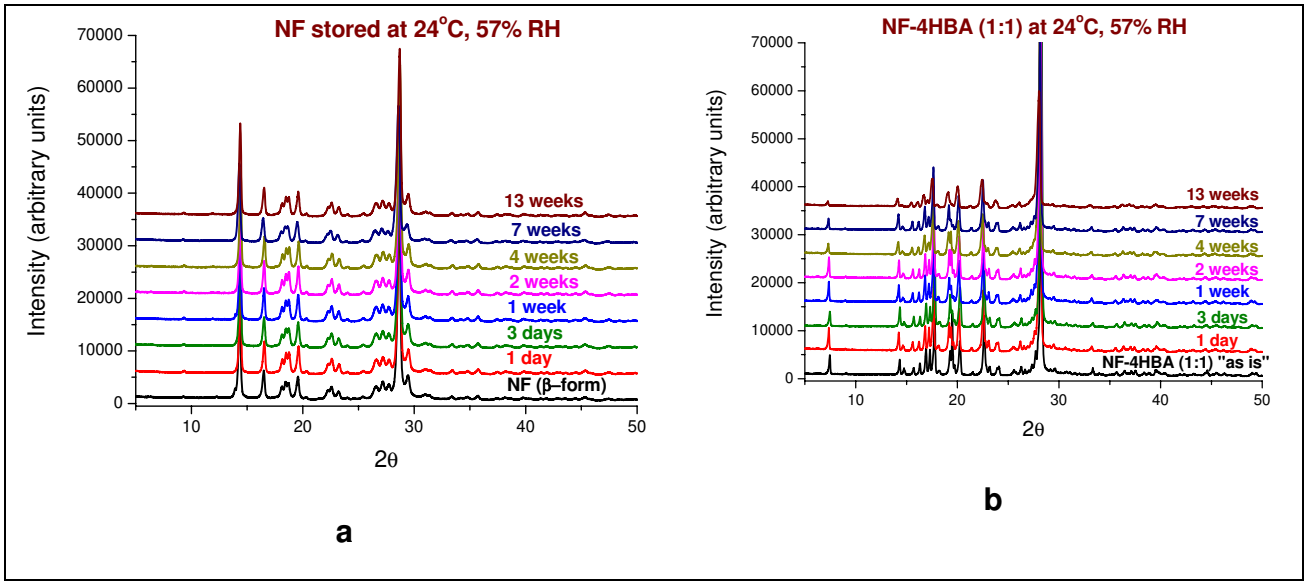

Fig. S14 (a) NF and (b) NF-4HBA (1:1) samples were incubated at 24 °C and 75% RH during 13 weeks. Product phases did not show detectable phase changes in PXRD.

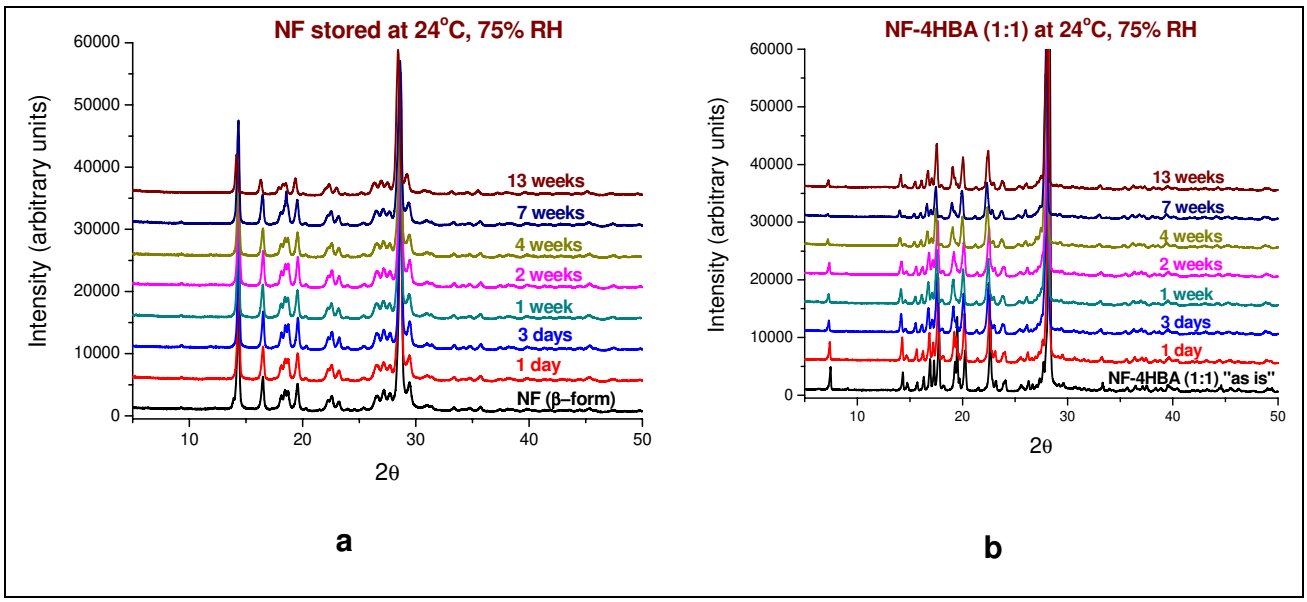

Fig. S15 (a) NF and (b) NF-4HBA (1:1) samples were incubated at 40 °C and 75% RH during 13 weeks. Product phases did not show detectable phase changes in PXRD.

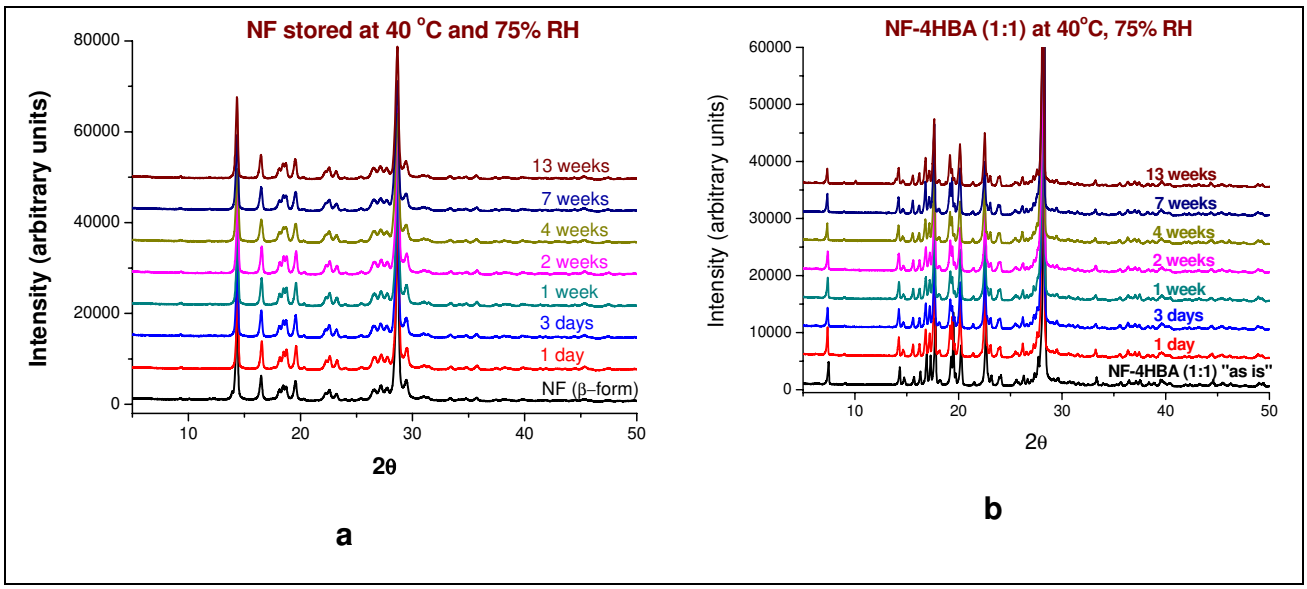

Fig. S16 (a) NF and (b) NF-4HBA (1:1) samples were incubated at 40 °C and 96% RH during 13 weeks. Notice NF (β-form) transformed to NF·H_2O (Form II) by 1 week, whereas NF-4HBA was stable for 13 weeks.

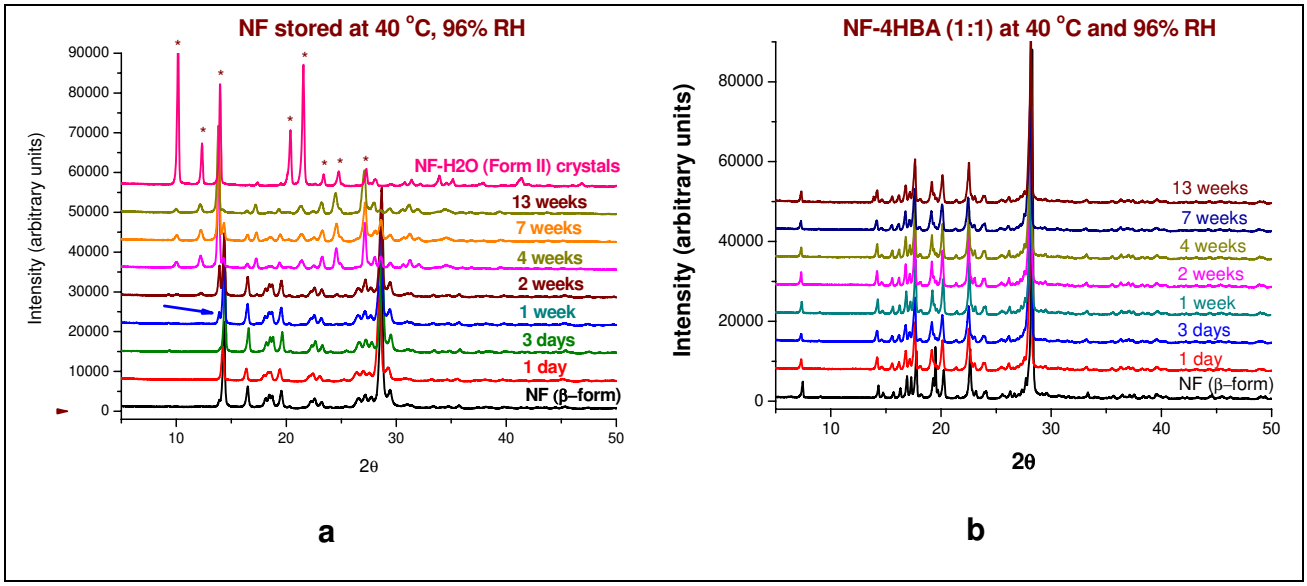

Fig. S17 NF and NF-4HBA (1:1) irradiated to UV light for 24 h and their product phase PXRD patterns were comparable to pure NF and NF-4HBA (1:1) indicates no noticeable new phases were observed at this degradation by PXRD.